Mine Closure 2026 – AB Fourie, G Boggs, J Heyes & M Tibbett (eds)

doi:10.36487/ACG_repo/2615_151

Using airborne electromagnetics to assess groundwater connectivity and ecological risk in a dewatered mine setting

Dilip Kumar [a], Daniel Hodges [b,*], Joanna Smallacombe [b]

[a] *Rio Tinto, Australia*

[b] *Geosyntec Consultants, Australia*

Abstract

Closure planning for an iron ore mine in the Pilbara incorporates protection of a woodland, classed as a protected ecological community (PEC). The PEC relies on a shallow aquifer, with mine operations dewatering a deeper aquifer. A thick clay aquitard separates the shallow and deeper aquifers; however, recent declining tree health has questioned the aquitard's continuity. Assessments in this area are complex and integrate within local cultural sensitivities requiring non-destructive methods. Hence, to assess the aquitard, a multiple lines of evidence study was initiated that integrated airborne electromagnetic (AEM) surveying, electrical resistivity imaging, borehole data, hydrogeological monitoring and ecological observations.

The AEM survey provided high-resolution mapping of shallow and deep subsurface conductivity, enabling improved delineation of key hydrostratigraphic units, particularly the clay aquitard. Results confirmed that the aquitard is laterally continuous beneath the PEC but thins or is absent to the north, indicating a potential zone of vertical hydraulic connection. This interpretation was strengthened through comparison with electrical resistivity imaging and available lithological logs. Furthermore, groundwater levels show a declining trend in the deep and shallow aquifers. Drawdown in the deep aquifer is associated with mine dewatering, while shallow groundwater levels fluctuate with long-term seasonal cycles primarily driven by large rainfall events associated with cyclonic activity and climate.

Although no direct hydraulic connection was detected, increased vertical gradients following dewatering create the potential for downward leakage in areas where the aquitard thins or is absent. Complementary evidence, including potential mine pit wall seepage, isotope datasets and ecological assessments, was included to holistically evaluate the factors influencing tree health.

The findings support development of mitigation options for closure to allow for shallow aquifer recharge. Overall, the multiple lines of evidence approach provided a robust foundation for closure planning by clarifying groundwater behaviour, risks and necessary future work.

Keywords: *airborne electromagnetics, groundwater-dependent ecosystems, aquitard integrity, mine dewatering, hydrogeological conceptual model*

1 Introduction

Open pit mining operations commonly require long-term dewatering to enable safe extraction below regional groundwater levels. While the impacts of dewatering on deep bedrock aquifers are typically well understood, there is often uncertainty regarding the effects on shallow groundwater systems and groundwater-dependent ecosystems located beyond the immediate mining footprint. This uncertainty is exacerbated in arid and semi-arid environments where rainfall recharge is episodic, monitoring datasets are sparse, access to sensitive receptors may be limited, and ecological systems may exhibit delayed or non-linear responses to hydrological change.

[*] Corresponding author: Email address: Daniel.hodges@geosyntec.com

In the study area considered in this paper, a PEC, within the semi-arid Pilbara region of Western Australia, is located within an internally draining basin adjacent to an active mine. Progressive vegetation decline had been observed over approximately a decade, prompting questions regarding potential links to mine dewatering, groundwater connectivity and reduced recharge associated with prolonged dry climatic conditions. Previous investigations relied primarily on sparse borehole data and limited ground-based geophysics, resulting in uncertainty with respect to the continuity of a key clay aquitard separating shallow and deep aquifers.

Airborne electromagnetic (AEM) surveying offers a non-invasive means of rapidly acquiring high-resolution subsurface conductivity data over large areas. When integrated with existing hydrogeological information, AEM data can significantly improve understanding of aquifer geometry, aquitard continuity and potential hydraulic pathways. This paper documents the application of AEM data in an operational mining context, with emphasis on environmental risk assessment rather than resource exploration.

2 Objective and scope of work

The primary objective of the geophysical investigation was to improve understanding of shallow and intermediate subsurface features that may influence hydrogeological conditions beneath a groundwater-dependent ecosystem (GDE) and the surrounding low-lying basin adjacent to an active mining operation. In particular, the study sought to address uncertainties in the existing conceptual hydrogeological model arising from limited site-specific subsurface data and to evaluate potential links between observed vegetation stress and regional groundwater drawdown associated with mine dewatering. Acknowledging the cultural and environmental sensitivities which prohibit ground-disturbance activities in the area, an AEM survey was undertaken, and the results were integrated into a broader geological and hydrogeological framework for the operation.

There were 3 specific aims of the survey. First, the study aimed to assess whether recent decline in vegetation condition within the ecological system could be attributed to groundwater drawdown caused by mining activities, either directly or via changes in hydraulic gradients. Second, the survey sought to test the consistency of geophysical results with the prevailing hydrogeological conceptual understanding of the basin, including the geometry and continuity of key hydrostratigraphic units. Third, the investigation sought to characterise the clay aquitard separating the shallow and deep hydrostratigraphic units beneath the GDE.

In addition to these core aims, the survey was intended to increase understanding of subsurface features that may influence groundwater flow paths, including the identification of potential recharge zones to deeper aquifers and the presence of structural features such as fractures and faults that could provide preferential hydraulic connectivity. Collectively, these aims were designed to support refinement of the site hydrogeological conceptual model and to inform closure considerations.

3 Study setting and hydrogeological context

3.1 Regional setting

The location of the study area is a semi-arid region of northwestern Australia characterised by high potential evaporation, episodic intense rainfall events and extended dry periods. The landscape comprises a low-relief sedimentary basin which lies at approximately 700 m Australian height datum, bound by elevated ridgelines underlain by Proterozoic bedrock units. Surface drainage is ephemeral, and groundwater represents the primary long-term water store supporting vegetation outside short post-rainfall periods.

Mining operations are located immediately south of the basin margin and have required sustained dewatering since the early 2010s. Groundwater extraction targets fractured bedrock units at depth and has resulted in regional drawdown.

3.2 Conceptual hydrostratigraphy

The hydrostratigraphic framework relevant to this study, as shown in Figure 1, consists of:

- a shallow, unconsolidated sedimentary aquifer responsive to rainfall recharge, specifically high-intensity rainfall events (e.g. cyclonic activity)
- an intermediate lacustrine clay aquitard of variable thickness
- a deeper fractured bedrock aquifer subject to mine dewatering.

Under pre-mining conditions, recharge to the deeper aquifer was conceptualised to occur primarily via rainfall infiltration along basin margins and exposed bedrock. The shallow aquifer was considered hydraulically separated from the deeper system across much of the basin by the clay aquitard. However, due to the lack of detailed studies due to the sensitivity of the area, uncertainty remained regarding localised thinning or absence of the clay unit in the greater part of the basin.

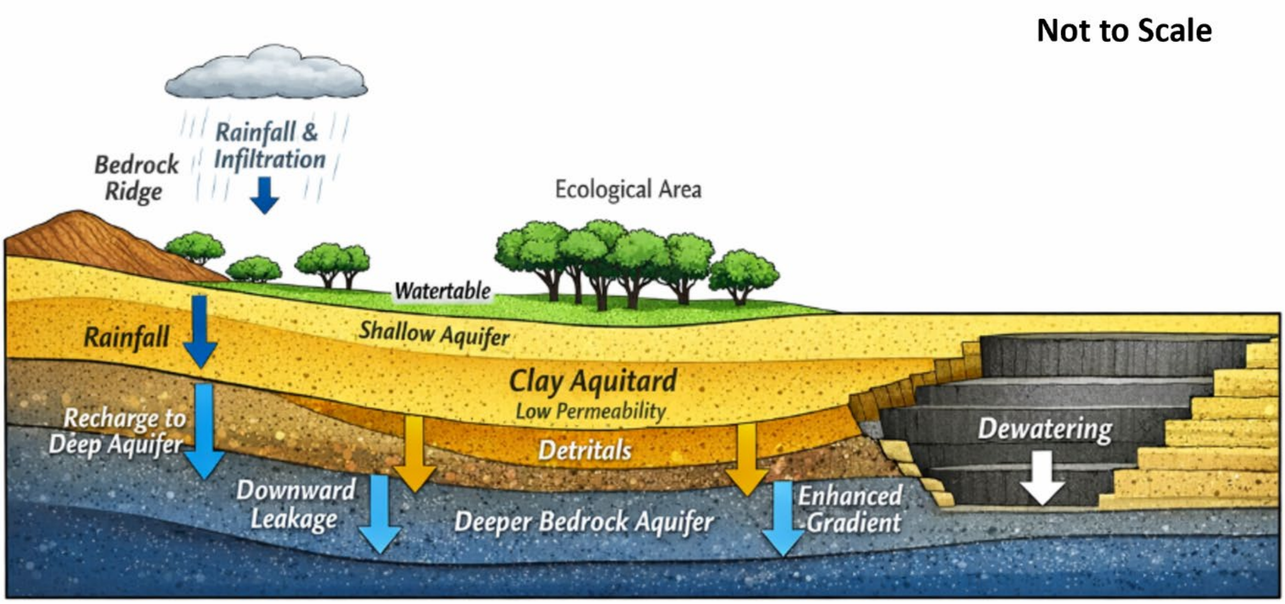

Figure 1 Conceptual site model showing groundwater flow paths

3.3 Climate and rainfall

Climate data for this study were sourced from SILO (developed by the Queensland Department of Energy and Climate). SILO uses climate data from the Bureau of Meteorology (BOM) and mathematical interpolations to develop climate datasets where direct observations are not available. The grid point representative of the Pilbara was used for this study.

The region is described as an arid-tropical climate with 2 distinct seasons: a hot humid summer from October to April and a relatively cooler winter from May to September, as shown in Figure 1. Temperatures are typically high, with summer averages frequently exceeding 40°C, while monthly winter averages between 23°C and 26°C.

Rainfall in the region can be highly variable due to the presence or absence of summer cyclones and thunderstorm activity; however, long-term annual averages of 357 mm are noted. Annual rainfall averages are also highly variable over longer timescales. Annual pan evaporation at the site is approximately 3,241 mm. Given the disparity between annual rainfall and annual evaporation, a net negative water balance is observed. Figure 2 displays the monthly average temperature, rainfall and pan evaporation over a 55-year period, highlighting that monthly pan evaporation exceeds monthly rainfall for each month of the year over the 1975–2025 time period.

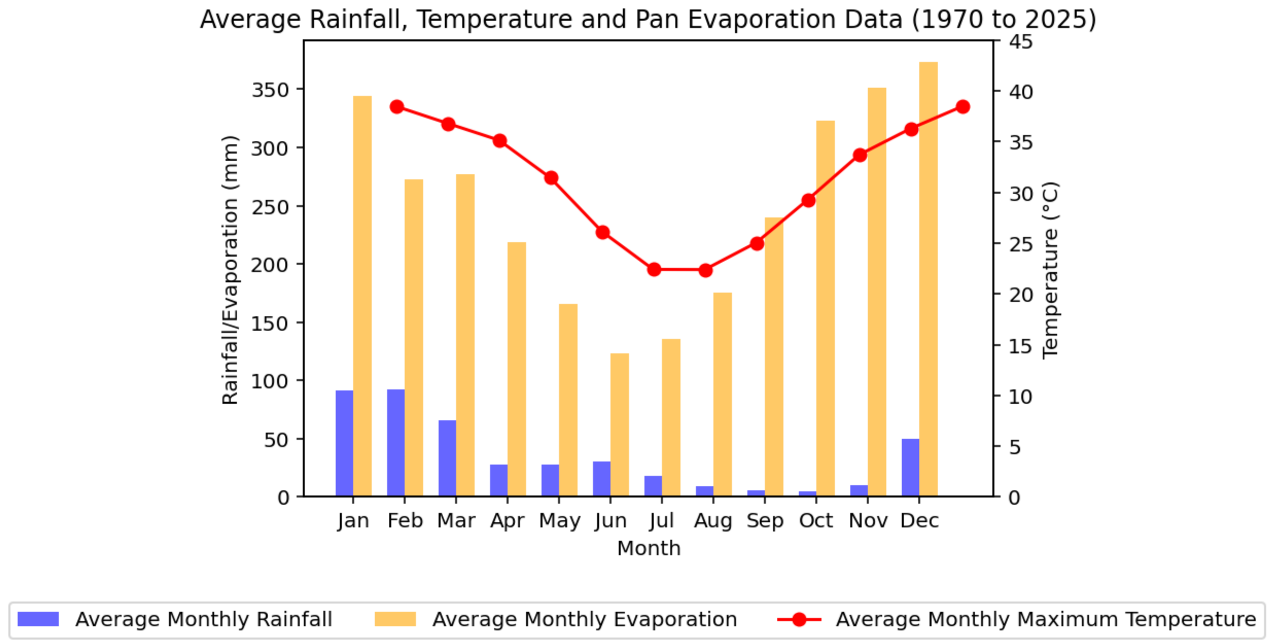

Figure 2 Average rainfall, temperature and pan evaporation data (1975–2025) (Source: SILO)

Over a 27-year period, the site has experienced changes in rainfall pattern (Figure 3). The cumulative departure from mean rainfall shows a drying trend from 1984 to 1997 which is promptly followed by a wet period of approximately 3 years (1998–2001). Fluctuations are noted proceeding this wet period, with an overall drying trend now being observed.

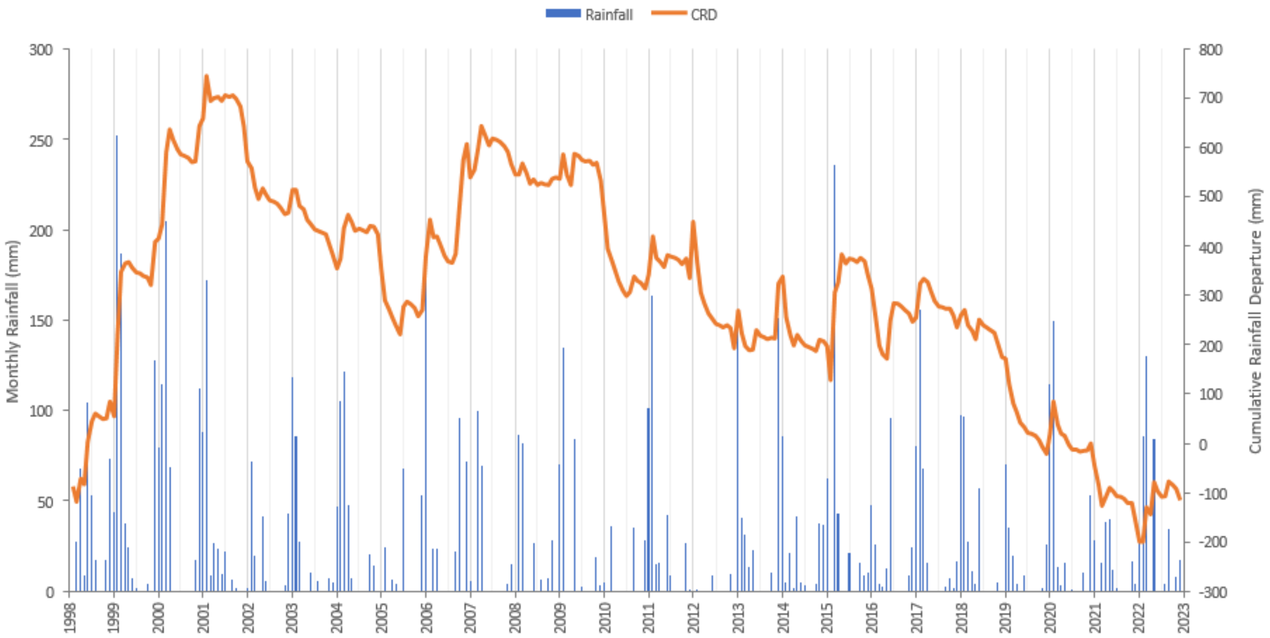

Figure 3 Monthly rainfall and cumulative rainfall departure (Source: BOM)

4 Methodology

4.1 Airborne electromagnetic survey design

The SkyTEM 306HP configuration consists of a hexagonal loop of approximately 68.3 m in circumference (i.e. surface area of 342 m^2) suspended below a helicopter. The loop generates an alternating current that produces an electromagnetic field that penetrates the Earth and creates secondary electric fields (eddy currents) in conductive material it passes through. The system operates using a dual-moment configuration, alternating between low moment (LM) and high moment (HM) transmitter pulses set at approximately 3,000 and 450,000 Am^2, respectively, to optimise both shallow resolution and depth of investigation. The secondary electric fields induce secondary magnetic fields, which are recorded by receivers mounted on frame flown approximately 30 m above the ground surface.

The receiver coils measure time-varying decay rate (dB/dt) of the magnetic field, which the system uses to derive the B-field. The system geometry and auxiliary measurements, including transmitter–receiver separation, loop orientation, frame tilt and altitude, were continuously monitored and incorporated into subsequent processing and inversion workflows, to ensure accurate reconstruction of the subsurface response.

The SkyTEM system was selected for this project due to its ability to its non-invasive nature, fast acquisition times and ability to resolve conductivity contrasts at various depths.

Survey design incorporated variable line spacing to balance resolution and spatial coverage as follows:

- high-resolution coverage across the GDE area (100 m spacing)
- broader regional coverage across the surrounding basin (500 m spacing).

A total of approximately 350 line-kilometres were acquired across 57 flight lines, across an area spanning 110 km^2.

4.2 Global positioning system data

The global positioning system (GPS) units are located on the front of the frame and positional information is therefore corrected to the centre of the frame. The corrected positions are translated into Transverse Mercator, GDA94 and MGA50.

4.3 Digital elevation model

A digital elevation model is derived using the laser positional information relative to the corrected GPS location. Pre-existing lidar data were used to quality check the GPS-generated digital elevation model from the survey and were found to compare well.

4.4 Electromagnetic data

Electromagnetic data collected during the survey were processed using SkyTEM proprietary software. This included the removal of cultural noise and spherics (i.e. outlier rejection) and estimation of noise-standard deviation throughout the survey area.

Interference between the generated and received signals which can affect the very early time data (i.e. magnetic field coupling from system bias) was hardware-monitored and later corrected using a stable primary field compensation technique. This process reduces the influence of the interference in the early time gates.

4.5 Data inversion

The processed SkyTEM electromagnetic data were inverted using spatially constrained inversion (SCI) implemented in Aarhus Workbench (developed at Aarhus University, Denmark) (Figure 4). The SCI approach simultaneously inverts multiple time-domain electromagnetic soundings[†] while applying lateral constraints

[†] A sounding refers to one data reading at a single point location, by multiple receiver channels, at varying times. Very early time readings generally relate to near surface responses, while later times relate to deeper responses.

between adjacent models both along and across flight lines, resulting in a quasi-3D conductivity model. This inversion framework balances resolution of laterally continuous geological features with suppression of spurious artefacts that may arise from isolated soundings.

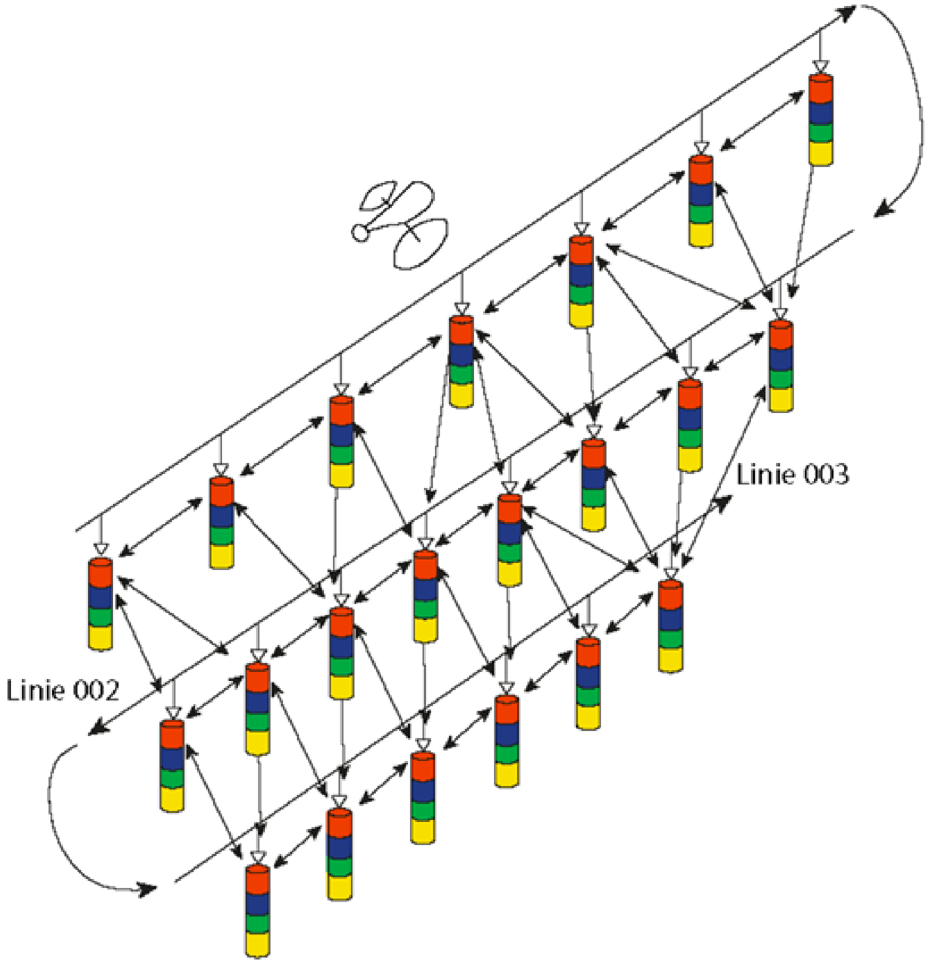

Figure 4 Schematic of SkyTEM inversion. Cylinders represent single-layered Earth models from individual data soundings, while arrows indicate model constraint directions

LM and HM transmitter data were inverted together within a single workflow to exploit the complementary strengths of each moment. The LM data provide high resolution in the near surface due to short turn-off times and early measurement gates, while the HM data offer increased depth of investigation through higher transmitter moments and improved signal-to-noise ratios at later times. Simultaneous inversion of both datasets enables robust characterisation of conductivity structure through a depth profile.

Automated data filtering was incorporated into the inversion workflow to exclude gates affected by excessive noise, negative voltages or coupling effects. Early time gates influenced by transmitter turn-off or residual primary field effects were omitted, as were late time gates with insufficient signal-to-noise ratios. Noise estimates derived during data processing were used to weight individual gates, ensuring that noisier data exerted less influence on the final model.

Depth of investigation (DOI) was calculated for each sounding based on sensitivity analysis of the Jacobian matrix from a 1D model (Christiansen & Auken 2012), providing an objective measure of the depth range over which conductivity estimates are supported directly by the data rather than by regularisation. Conductivity values below the DOI are therefore considered increasingly uncertain and were interpreted with caution. Model quality was further assessed using data residuals, defined as the misfit between observed and model-predicted responses. Elevated residuals commonly occur where strong lateral conductivity contrasts, cultural interference, or 3D geological effects violate the 1D inversion assumption.

The final inversion results were delivered as conductivity section profiles, gridded conductivity depth slices, and model databases suitable for 3D geological and hydrogeological interpretation. These products form the basis for subsequent assessment of stratigraphic architecture, aquitard continuity and potential groundwater connectivity across the survey area.

4.6 Geology model

A geological model was developed using Seequent Leapfrog software. The conductivity section profiles provided by SkyTEM were imported into Leapfrog and the layer boundaries (identified by conductivity contrasts) were delineated manually using polygons. The polygons were used to generate surfaces for each layer interface. These surfaces were then brought into the geology model and used to create 3D volumes for each formation. Formations that were not continuous along each section and did not intersect the surface or base of section were modelled as intrusions, while the other formations were modelled as deposits. Two separate models were created – one for the ecological community, and one for the overall basin. This allowed the area with the ecological community to modelled with a finer resolution due to the closer line spacing.

The purpose the geology model was to help identify the following:

- outcropping formations that may indicate aquifer recharge zones
- areas where the clay layer is not present and could indicate connectivity between shallow and deep aquifers
- extent, depth and thickness of clay layer
- extent, depth and extent of aquifers
- depth and distribution of deeper conductive layer.

4.7 Integration with existing datasets

AEM outputs were interpreted alongside:

- historical groundwater monitoring data from shallow and deep bores
- available borehole lithology logs
- previously acquired ground-based electrical resistivity imaging.

This integrated approach ensured that conductivity interpretations were grounded in known geological and hydrogeological conditions.

5 Results

5.1 Geology

The outputs provided by SkyTEM allowed for interpretation of geology across the assessment area. For these outputs, the geology models are represented by conductivity values, as reported by SkyTEM. For these models, higher conductivity values are shown as orange and red while lower conductivities are shown in green to blue. The conductivity outputs are shown on figures presented in sections 5.2 and 5.3.

5.2 Conductivity depth sections

The conductivity depth maps show the inverted conductivity for each of the model layers (1–30). The thicknesses of each depth slice increase with depth and the maps represent the conductivity across each thickness interval. Depth slices are shown in Figures 5–12.

The AEM survey resolved 3 primary conductivity domains consistent with the conceptual hydrostratigraphic framework. Near-surface resistive zones correspond to unsaturated sediments and shallow aquifer materials, underlain by a variably conductive intermediate layer interpreted as lacustrine clay. At depth, lower conductivity units correspond to fractured bedrock aquifers.

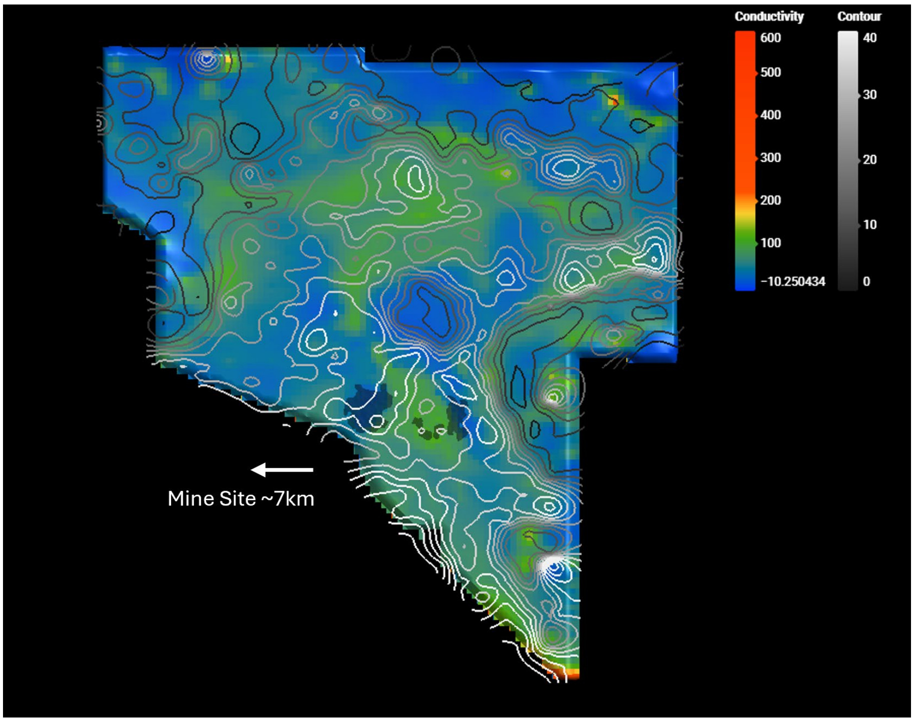

Figure 5 Conductivity depth slice, 10.0–14.1 m bgl, overlain with clay thickness contours

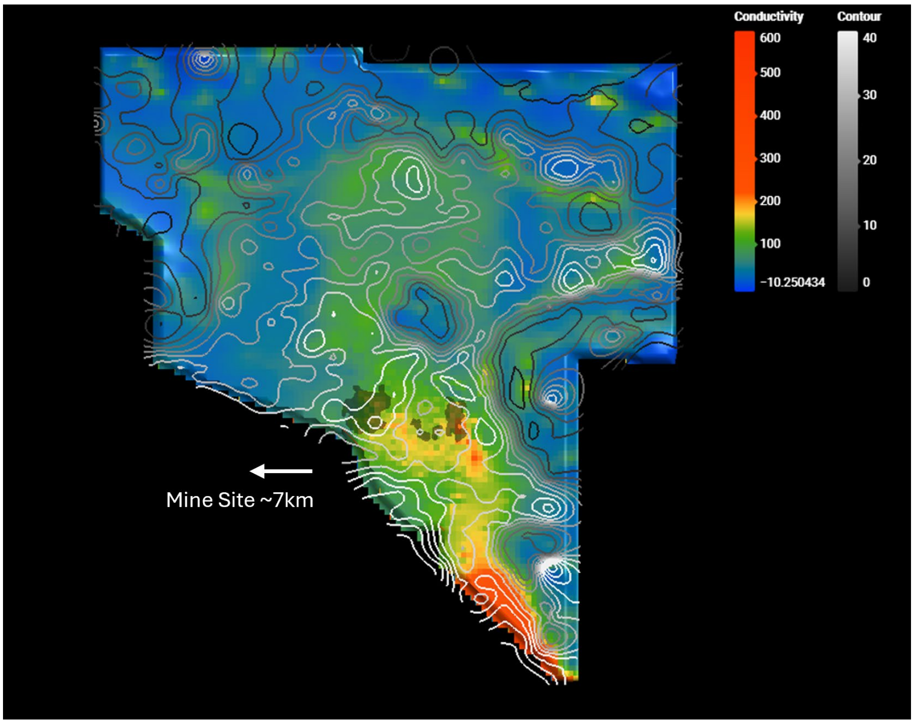

Figure 6 Conductivity depth slice, 14.1–18.6 m bgl, overlain with clay thickness contours

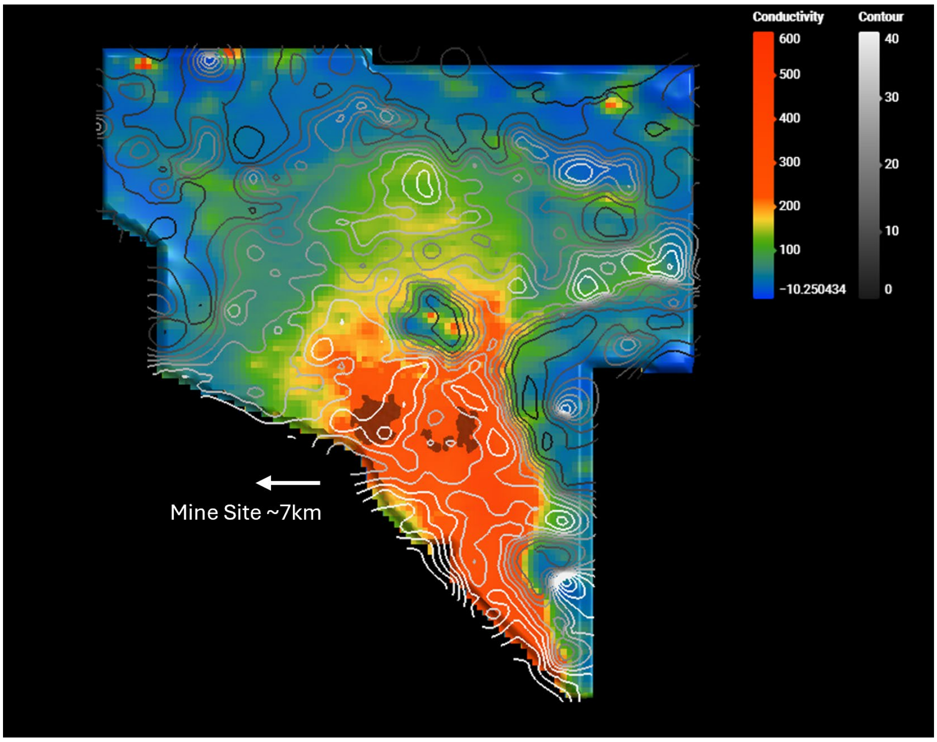

Figure 7 Conductivity depth slice, 23.5–29.0 m bgl, overlain with clay thickness contours

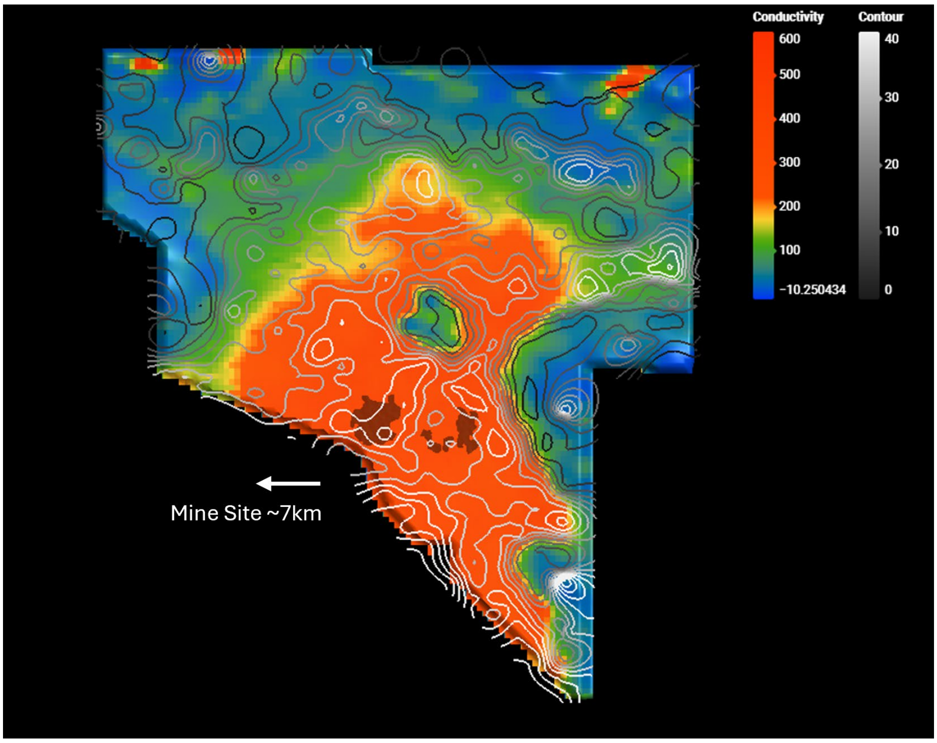

Figure 8 Conductivity depth slice, 29.0–35.1 m bgl, overlain with clay thickness contours

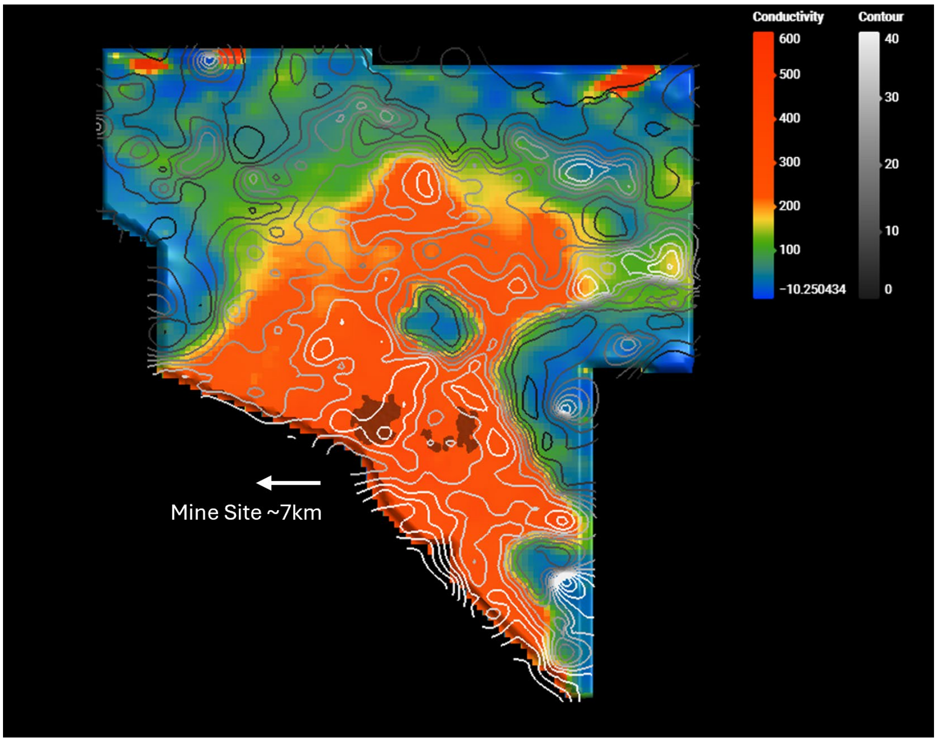

Figure 9 Conductivity depth slice, 35.1–41.8 m bgl, overlain with clay thickness contours

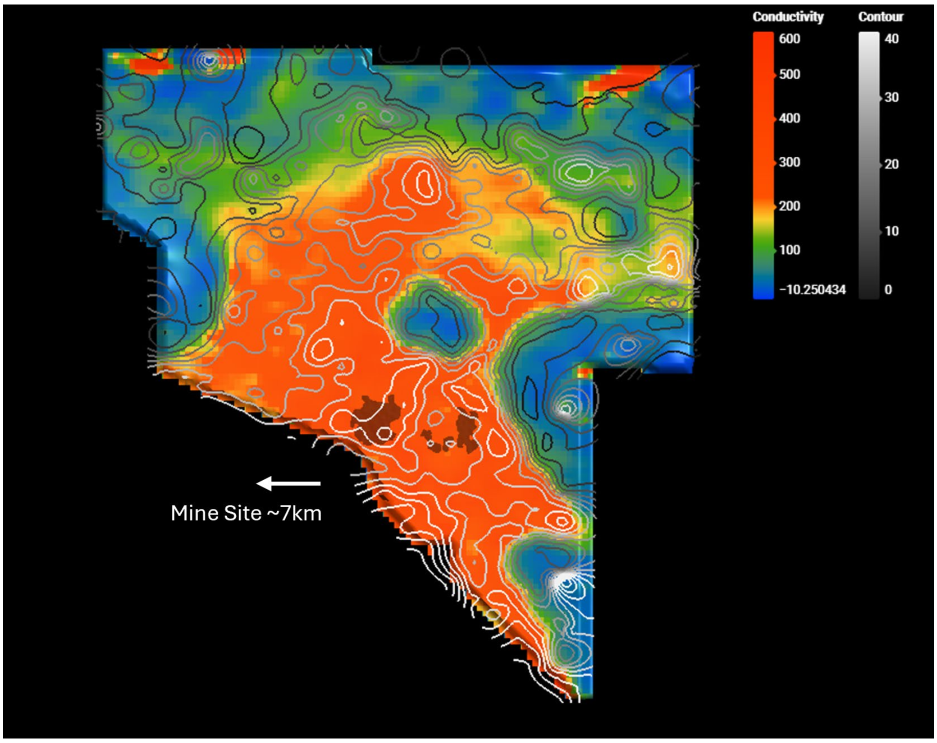

Figure 10 Conductivity depth slice, 41.8–49.3 m bgl, overlain with clay thickness contours

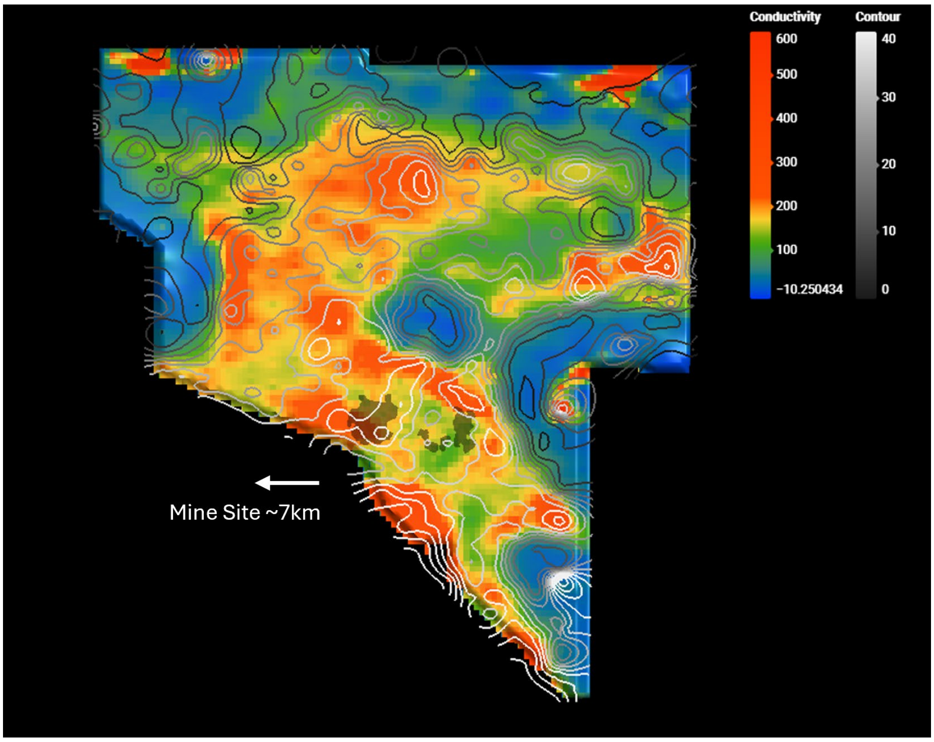

Figure 11 Conductivity depth slice, 49.3–57.5 m bgl, overlain with clay thickness contours

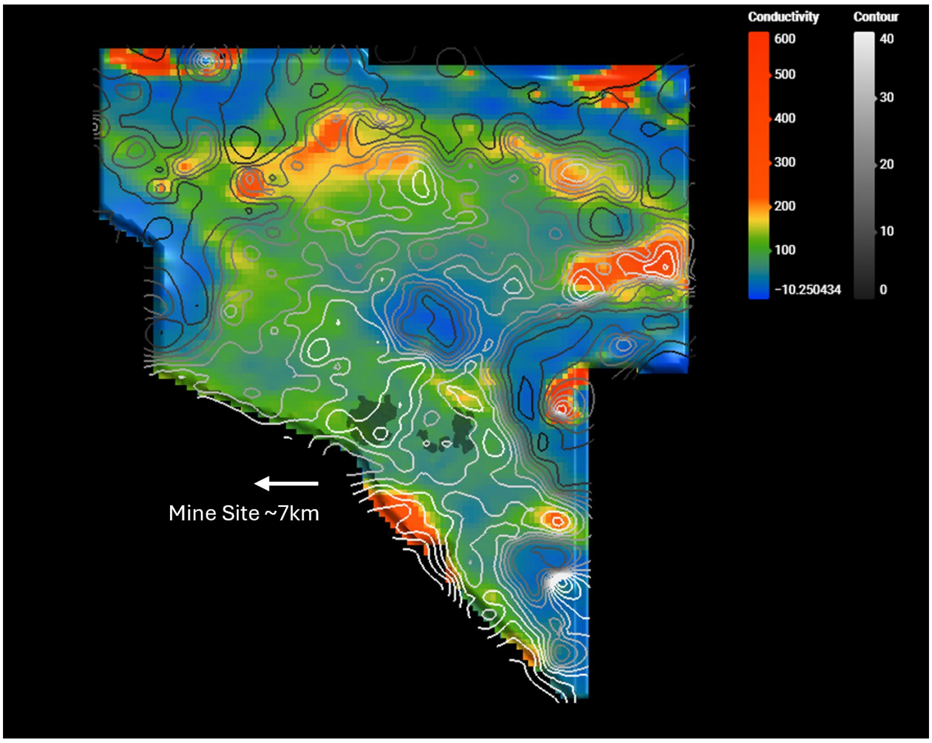

Figure 12 Conductivity depth slice, 57.5–66.6 m bgl, overlain with clay thickness contours

5.3 Conductivity section profiles

The profile plots provided by SkyTEM are provided for each flight line and consist of 4 sections. The top section shows the inverted conductivity profile along the line, with the conductivity shown on a logarithmic scale. The thin grey line indicates the upper DOI and the white shading in the analysis section indicates the estimated DOI. The blue line above the conductivity section shows the flight elevation (frame height). The second and the third profile plots show the measured data that were imported into Workbench (faint grey profiles), the measured data that were included in the Workbench inversion (coloured dots), and the calculated response of the inverted models (solid coloured lines) for low moment data (LMZ) and high moment data (HMZ). Areas containing only the faint grey profile lines indicate data that were excluded from the inversion due to poor quality, e.g. a low signal-to-noise ratio. An example of the SkyTEM section profiles is shown in Figure 13.

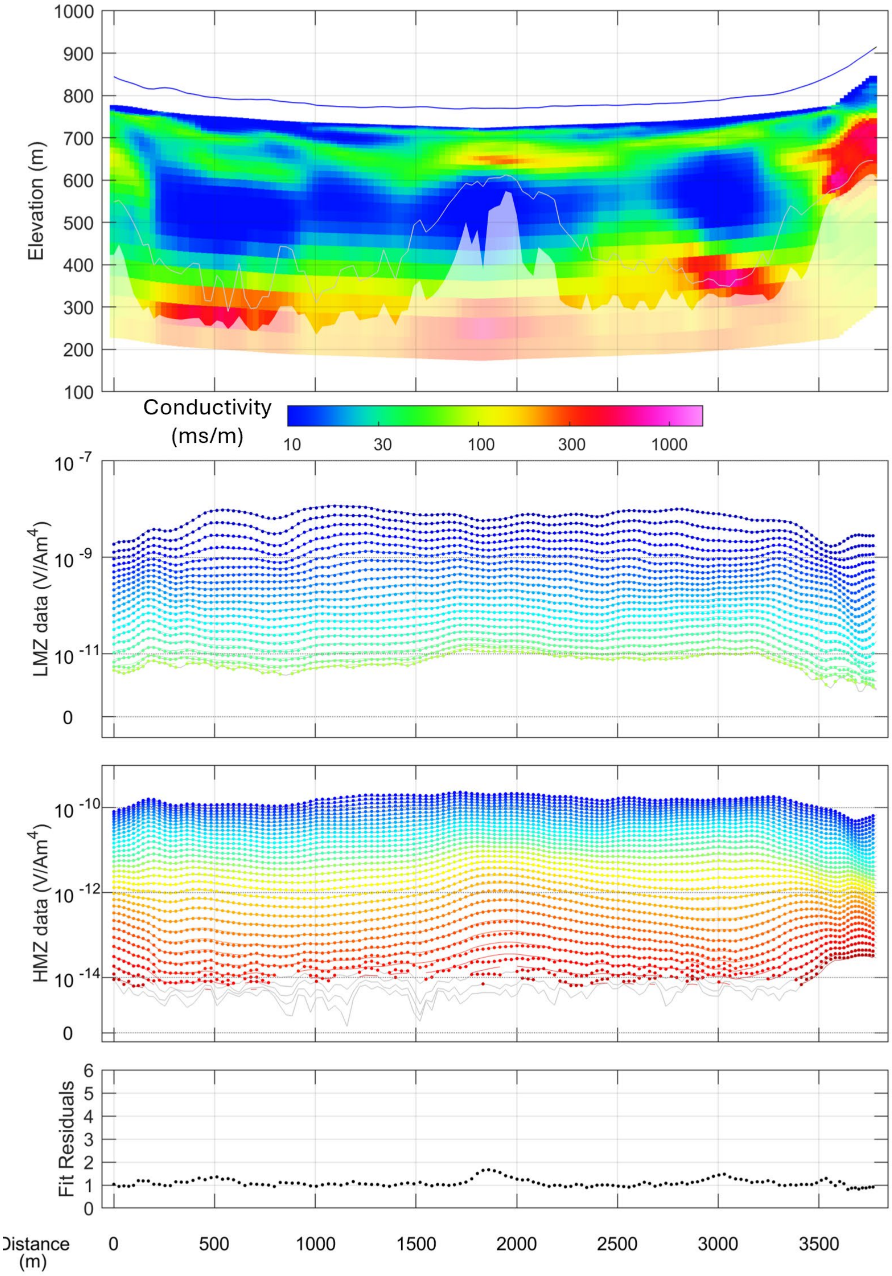

Figure 13 Example of a SkyTEM conductivity section profile (top), low moment and high moment data (second and third from top) and data residuals (bottom)

6 Discussion

6.1 Geology models

Based on borehole logs for the area and other regional geological characteristics, the interpreted geological units from the conductivity profiles approximately align with the known regional geological units for the area of investigation. However, as there are limited drilling locations across the broader investigation area, it is acknowledged that the boundaries between units are inferred and would require confirmation through intrusive investigations.

6.1.1 Aquitard continuity beneath the ecological receptor

Across the PEC, the clay aquitard is interpreted to be laterally continuous, with thickness generally in the 10–60 m range. No significant thinning, breaches, or conductive anomalies indicative of preferential vertical flow pathways were identified beneath this area.

6.1.2 Basin margin connectivity and recharge zones

In contrast, conductivity depth slices indicate thinning or local absence of the clay unit at the margins of the broader basin, particularly adjacent to elevated bedrock ridgelines. These areas coincide with conceptual groundwater recharge zones and likely represent locations where vertical hydraulic connectivity between shallow and deep systems may occur under natural conditions.

6.2 Comparison with groundwater level trends

Shallow groundwater monitoring data indicate strong responsiveness to major rainfall events but an overall declining trend since approximately 2010. Deep groundwater levels show sustained decline consistent with dewatering, with minimal response to rainfall. The divergence between shallow and deep trends supports the interpretation of effective hydraulic separation beneath the ecological receptor, despite increased vertical gradients.

6.3 Implications for ecohydrological risk

The AEM results do not support a mechanism whereby mine dewatering directly intercepts groundwater beneath the PEC. Instead, influence of dewatering on the shallow system is likely indirect and mediated through regional groundwater redistribution or basin margin leakage.

6.4 Role of climate variability

Climate data indicate below-average rainfall conditions over much of the past 2 decades. Reduced recharge frequency and magnitude are likely to have diminished shallow groundwater availability, contributing to vegetation stress independently of mining activities.

6.5 Value of airborne electromagnetic surveys for environmental assessment

This study demonstrates that AEM surveys are a powerful tool for reducing uncertainty in environmental risk assessments involving interpretation of ecohydrological systems at mine sites. While ground-based methods provide superior near-surface resolution, AEM data uniquely enable basin-scale interpretation of delineating hydrogeological features.

6.6 Limitations

The AEM resolution used in this study was insufficient to reliably detect small-scale features such as sinkholes or narrow fractures. Where such features are of concern, targeted ground-based techniques could be used to delineate and identify them.

7 Conclusion

The AEM survey significantly improved understanding of groundwater connectivity beneath a protected ecological receptor adjacent to an active mine. Results confirm continuous aquitard separation beneath the ecological area and identify basin margin recharge zones where vertical connectivity is more likely. Vegetation decline is interpreted to be driven primarily by climatic factors, potentially compounded by regional hydrogeological changes rather than direct localised dewatering impacts. The approach provides a defensible framework for integrating geophysics into mine environmental management and closure planning.

Acknowledgement

The authors acknowledge the support of site environmental and hydrogeology teams involved in data collection, interpretation workshops and technical review. Key personnel include Laura Tan, Matthew Lawrence and Mahtab Rashidifard from Rio Tinto, and Joanna Smallacombe from Geosyntec.

References

Christiansen, AV & Auken, E 2012, 'A global measure for depth of investigation', *Geophysics*, vol. 77, no. 4.